




# A Two-Stage Cooperative Multi-objective Evolutionary Differential Algorithm for Combined Heat and Power Economic Emission Dispatch

Chaodong Fan<sup>1,2,3,4</sup> · Yuetang Wu<sup>1,3,4</sup> · Hongbo Hu<sup>1</sup> · Leyi Xiao<sup>2,4,5,6</sup>  · Lingzhi Yi<sup>1,3</sup> · Xiaoqing Ning<sup>7</sup>

Received: 11 February 2022 / Accepted: 29 June 2022 / Published online: 3 August 2022  
© King Fahd University of Petroleum & Minerals 2022

## Abstract

Combined heat and power economic emission dispatch (CHPEED) can obtain good economic and environmental benefits, but the dispatch problem presents non-convex, nonlinear, multi-constrained and multi-objective characteristics. Thus, a two-stage cooperative multi-objective differential evolutionary algorithm (TCADEA) is proposed in this paper. The algorithm uses a two-stage framework: the first stage uses a two-population strategy to divide the population into an elite population and an ordinary population, where the elite population is used to obtain better target values and the ordinary population is used to search the target space to ensure the diversity of the population and update the two populations by different adaptive differential operators. In addition, the  $\varepsilon$  constraint processing technique is used to handle the constraints. The second stage combines two populations into one and generates offspring through the constrained dominance principle (CDP) and adaptive differential evolution to maintain well-distributed population. The actual case results show that the TCADEA algorithm reduces  $\$0.034 \times 10^6$ ,  $\$0.008 \times 10^6$ ,  $\$0.07 \times 10^6$  and  $113 \times 10^5$  lb,  $102 \times 10^5$  lb,  $155 \times 10^5$  lb in fuel cost and emissions compared to MODE, NSGA-II, and TOP, respectively.

**Keywords** Economic emission dispatch · Cogeneration · Adaptive differential evolution · Dual-population framework · Multi-objective optimization

## 1 Introduction

Generating units using fossil fuels often have low efficiency and high pollution during power generation [1], so both must

be considered in engineering applications [2]. At present, even in the state-of-the-art combined cycle power plants, the energy conversion efficiency is only between 50 and 60% [3]. To improve the efficiency of the use of existing power systems, combined heat and power unit (CHP) was introduced [4]. CHP enables effective control of operating cost and pollution emissions [5, 6]. However, some references only consider the optimization of the economic aspects of CHP, ignoring the environmental advantages of the unit [7–9]. With the increasingly serious environmental problems, many countries around the world are actively working on energy saving and emission reduction. The economic emission dispatch as an effective way to cope with the energy crisis and environmental pollution. The purpose is to ensure reliable power supply while balancing economic efficiency and pollutant emissions, thus achieving safe and stable operation of the power system with the lowest operating costs and minimal pollution emissions [10].

The solution methods for multi-objective economic emission dispatch problems are usually divided into two types: traditional mathematical methods and heuristic algorithms. In many literatures, traditional mathematical methods are

✉ Leyi Xiao  
xiaolytkx@163.com

<sup>1</sup> College of Automation and Electronics Information, Xiangtan University, Xiangtan 411105, China  
<sup>2</sup> School of Information Technology and Management, Hunan University of Finance and Economics, Changsha 410205, China  
<sup>3</sup> Foshan Green Intelligent Manufacturing Research Institute of Xiangtan University, Foshan 528000, China  
<sup>4</sup> School of Computer Science and Technology, Hainan University, Haikou 570228, China  
<sup>5</sup> Fujian Provincial Key Laboratory of Data Intensive Computing, Quanzhou Normal University, Quanzhou 362000, China  
<sup>6</sup> Vehicle Measurement, Control and Safety Key Laboratory of Sichuan Province, Xihua University, Chengdu 610039, China  
<sup>7</sup> School of Big Data and Computer Science, Shanxi Institute of Science and Technology, Jincheng 048012, China



widely used in CEED and CHPEED, such as  $\lambda$  iteration [11], Newton–Raphson method [12], and Lagrangian multiplier method [13]. Since economic emission dispatch has high-dimensional, nonlinear, discontinuous, and non-differentiable characteristics, traditional mathematical methods often fall into local optimum or converge prematurely, making it difficult to obtain a set of optimal Pareto fronts (PF). In contrast, heuristic algorithms are empirical-based optimization methods, so they are widely used in high-complexity optimization problems such as artificial intelligence and production dispatching, such as dwarf meerkat optimization algorithm (DMO) [14], crawl search algorithm (RSA) [15], and arithmetic optimization algorithm [16]. Heuristic algorithms are a simple and effective solution for economic emission dispatch problems with valve point effects and feasible operating zones [17, 18]. To solve the CEED problem, Koridak et al. used weight coefficients to transform the bi-objective optimization problem into a single-objective optimization problem, which can lead to optimization results that depend on the setting of the weight coefficients [19]. Abdelaziz et al. used a switching factor  $p$  to determine the global and local search of the flower pollination algorithm (FPA) with a  $p$  value that is biased towards local search, which can lead the population to fall into a local optimum [20]. In reference [21], the ant colony optimization (ACO) combined with the ratio of maximum fuel cost and emissions transforms the CEED problem into an economic optimization problem, which reduces the optimization difficulty. Because fuel cost and emissions are nonlinear functions whose weight varies with the output power of the generator set, it is not reasonable to use a fixed ratio of fuel cost to emissions. A new symbiotic organisms search algorithm (NSOS) is used to solve the CEED problem with an algorithm that generates complementary terms for individuals that do not guarantee a priori an improvement in algorithm performance [22]. Sharifi et al. proposed a price penalty function to balance the relationship between economy and emissions and solved the CEED problem by spiral optimization algorithm (SOA). This method can obtain the optimal solution quickly, but the maximum capacity of each generating unit differs, which can lead to large or small emissions of other generating units when the price penalty factor is multiplied with the emissions of other generating units [23]. A gravity-based artificial bee colony algorithm is used to solve the CEED problem. The mathematical model developed in this literature is not practical because its objective function does not take into account the valve point effect of the generating unit, which can cause huge fluctuations in the output power of the generating unit [24].

The above solution methods all convert the CEED problem into a single objective for optimization by the weighting

method. This method relies heavily on the reasonable assignment of weight coefficients, and it is often difficult to obtain a suitable weight without a priori knowledge. Therefore, the use of multi-objective optimization algorithms to solve such problems is a current research hotspot. In solving the CHPEED problem, NSGA-II is used to solve the CHPEED problem. Although it converges quickly to the PF, there are too few test systems and comparison algorithms to fully validate the effectiveness of NSGA-II on the CHPEED problem [25]. A particle swarm algorithm with time-varying acceleration coefficients (TVAC-PSO) is used to deal with this problem. It combines an originally fixed acceleration factor with the number of iterations to prevent the algorithm from falling into a local optimum [26]. An Indicator & crowding Distance-based Evolutionary Algorithm (IDBEA) increases the diversity of solutions in solving the CHPEED problem, but the performance of the method is heavily dependent on the setting of reference points [27]. A two-stage optimization approach is proposed in the reference [28], which first uses a multi-objective optimization algorithm based on  $\theta$  domination for optimization and then selects the best compromise solution by an integrated decision-making approach. Since  $\theta$  values do not use adaptive techniques, this can lead to the need for multiple solutions to determine the appropriate  $\theta$  value when solving the problem.

However, the above approach to solving the CHPEED problem focuses only on how to minimize the economic emission target and does not study much about the constraints in this problem. In order to solve the problem of multi-objective and multi-constraint, a multi-objective multi-verse optimization algorithm based on a chaotic opposition strategy is proposed. And the combination of constraint processing technique ensures that the solution is in the feasible zones [29]. In the reference [30], a multi-objective line-up competition algorithm (MLCA) with diversity mechanism and constraint processing technique is proposed to solve the CHPEED problem considering valve point effect and transmission loss. In general, constraint processing techniques can be divided into repair strategy, penalty function, and rejection strategy. The repair strategy obtains individuals that satisfy the constraints by multiple cycles, and its optimization process is complex. The penalty function adds the constraint violation value to the objective function by the penalty factor, and it is very dependent on the value of the penalty factor. The rejection strategy selects the superior individual by comparing the constraint violation values of two individuals, and this strategy is simple and effective. The constraint processing techniques proposed in references [29, 30] are based on the repair approach. Therefore, a two-stage cooperative multi-objective evolutionary differential algorithm incorporating rejection strategy is proposed to solve the CHPEED

problem in this study. The method is divided into two stages: the first stage uses a dual-population strategy, in which two populations use different adaptive differential operators and obtain offspring according to the  $\varepsilon$ -constrained processing technique and the Pareto principle to ensure that the population gets more superior individuals; in the second stage, to ensure a more uniform PF for the economic emission dispatch problem, the elite population and ordinary population are combined into one population and evolve according to the adaptive differential operator and CDP. The experimental results of CEED and CHPEED show that the TCADEA algorithm is able to obtain solutions with better distributivity.

The main contributions of this article are as follows:

1. A two-stage cooperative multi-objective evolutionary differential algorithm (TCADEA) is proposed. The method uses a two-stage framework for optimization. The first stage uses a dual-population mutation strategy to generate offspring and then updates the solution through an  $\varepsilon$ -constraint processing technique. For example, the dual-population strategy generates offspring through adaptive differential operators, and the  $\varepsilon$ -constrained processing technique selects the next generation of populations through  $\varepsilon$ -constrained non-dominated sorting. The second stage obtains offspring by single-population optimization and CDP. For example, elite population and ordinary population are combined into a single population to obtain offspring by differential operator, and then the next-generation population is obtained by environmental selection according to CDP.
2. The CEED and CHPEED problems with valve point effect and transmission loss are solved.
3. The simulation experiments are performed for the CEED problem and the CHPEED problem. TCADEA obtained better results on four cases compared to MODE, NSGA-II and TOP. For example, in Case 4, the TCADEA algorithm reduces  $\$0.034 \times 10^6$ ,  $\$0.008 \times 10^6$ ,  $\$0.07 \times 10^6$  and  $113 \times 10^5$  lb,  $102 \times 10^5$  lb,  $155 \times 10^5$  lb in fuel cost and emissions compared to MODE, NSGA-II, and TOP, respectively.

The rest of this paper is organized as follows. Section 2 introduces two typical models of economic emission dispatch problems: the CEED problem and the CHPEED problem. Section 3 describes the overall framework of the algorithm and gives the implementation details of the algorithm. Section 4 is a comparative experiment, comparing and analyzing the advantages and disadvantages of the proposed algorithm and other algorithms. Section 5 summarizes the main work of this article.

## 2 Economic Emission Dispatch Problem

Economic emission dispatch problems are roughly divided into CEED problems and CHPEED problems. They are a multi-objective dispatch problem that minimizes fuel cost and pollution emissions while satisfying multiple constraints. The general multi-objective problem model is as follows:

$$\begin{aligned}
 \min F(x) &= [F_1(x), F_2(x)] \\
 s.t. g(x) &= [g_1(x), g_2(x), \dots, g_K(x)] \leq 0 \\
 h(x) &= [h_1(x), h_2(x), \dots, h_M(x)] = 0 \\
 x &= [x_1, x_2, \dots, x_d, \dots, x_D] \\
 x_d^{\min} &\leq x_d \leq x_d^{\max}, (d = 1, 2, \dots, D)
 \end{aligned} \tag{1}$$

where  $F_1(x)$  and  $F_2(x)$ , respectively, represent operating cost and pollution emission,  $g(x)$  represents k-term inequality constraint,  $h(x)$  represents M-term equality constraint,  $X$  represents output power of  $D$  generator unit, and  $x_d^{\min}$  and  $x_d^{\max}$  represent upper and lower limits of output power of each unit.

### 2.1 Formulation of CEED Problem

#### 2.1.1 Objective Function

In the real power generation process, the plucking phenomenon caused by the sudden opening of the turbine inlet valve will cause the pulsation effect of the unit consumption characteristics, i.e., the valve point effect [31]. In order to ensure the accuracy of solving the CEED problem, the valve point effect should be considered when establishing the mathematical model of the problem.

The fuel cost of the generator unit is shown in Eq. (2).

$$F_1(x) = \sum_{i=1}^{M_p} a_i P_i^2 + b_i P_i + c_i + \left| d_i \sin \left\{ e_i \left( P_i^{\min} - P_i \right) \right\} \right| \tag{2}$$

where  $|d_i \sin \{e_i (P_i^{\min} - P_i)\}|$  represents the valve point effect,  $e_i$  and  $d_i$  represent the cost coefficient of the  $i$ th power-only unit,  $P_i^{\min}$  represents the minimum output power of the  $i$ th power-only unit,  $P_i$  represents the actual output power of the  $i$ th power-only unit,  $a_i, b_i, c_i$  represent the cost coefficient of the  $i$ th power-only unit, and  $M_p$  represents the number of power-only units.

When fossil fuels are used for power generation, the power generation system produces various harmful gases that pollute the environment (here mainly  $NO_x, SO_x, CO_2$ ). The emissions are shown as follows:

$$F_2(x) = \sum_{i=1}^{M_p} g_i P_i^2 + h_i P_i + k_i + n_i e^{l_i P_i} \tag{3}$$

where  $g_i, h_i, k_i, l_i$  represent the emission coefficient of the  $i$ th power-only unit.

### 2.1.2 Constraints

In the CEED problem, the energy balance constraint and the power constraints of each unit are considered mainly, which are summarized as follows.

The power generated by the unit is equal to the sum of the power required on the load side plus the transmission losses between the units.

$$\sum_{i=1}^{M_p} P_i = Pd + Pl \tag{4}$$

where  $Pd$  represents the electricity demand on the load side. Transmission loss  $Pl$  is shown by Eq. (5).

$$Pl = \sum_{i=1}^{M_p} \sum_{j=1}^{M_p} P_i P_j B_{ij} + \sum_{i=1}^{M_p} B_{0i} P_i + B_{00} \tag{5}$$

where  $B_{ij}$  represents the loss coefficient between the  $i$ th power-only unit and the  $j$ th power-only unit,  $B_{0i}$  represents the loss coefficient of the  $i$ th power-only unit, and  $B_{00}$  represents the loss coefficient parameter.

Power constraints of each unit.

$$P_i^{\min} \leq P_i \leq P_i^{\max}, \quad i = 1, 2, \dots, M_p \tag{6}$$

where  $P_i^{\min}$  and  $P_i^{\max}$ , respectively, represent the minimum power and maximum power of the  $i$ th power-only units.

## 2.2 Formulation of CHPEED Problem

### 2.2.1 Objective Function

The CHPEED problem results in better operating cost and emissions of the power generation system due to the incorporation of CHP [32]. The fuel cost function and emission function of the CHPEED problem are added to the fuel cost and emission of the CHP and the heat-only unit. The expressions are shown in Eqs. (7) and (8).

$$F_1(x) = \sum_{i=1}^{M_p} C_{p,i}(P_i) + \sum_{j=1}^{M_c} C_{c,j}(O_j, H_j) + \sum_{n=1}^{M_h} C_{h,n}(T_n) \\ = \sum_{i=1}^{M_p} a_i P_i^2 + b_i P_i + c_i + |d_i \sin\{e_i (P_i^{\min} - P_i)\}|$$

$$+ \sum_{j=1}^{M_c} [\alpha_j O_j^2 + \beta_j O_j + \chi_j + \varphi_j H_j^2 + \gamma_j H_j + \eta_j O_j H_j] \\ + \sum_{n=1}^{M_h} [t_n T_n^2 + \kappa_n T_n + \lambda_n] \tag{7}$$

where  $C_{p,i}, C_{c,j}, C_{h,n}$ , respectively, represent the fuel cost of the  $i$ th power-only unit, the  $j$ th CHP unit and the  $n$ th heat-only unit.  $P_i$  represents the actual power generation of the  $i$ th power-only unit,  $O_j$  represents the actual power generation of the  $j$ th CHP unit,  $H_j, T_n$  respectively represent the actual heat production power of the  $j$ th CHP unit and the  $n$ th heat-only unit,  $\alpha_j, \beta_j, \chi_j, \varphi_j, \gamma_j, \eta_j$  represent the cost coefficients of the  $j$ th CHP unit, and  $t_n, \kappa_n, \lambda_n$  represent the cost coefficients of the  $n$ th heat-only unit.

$$F_2(x) = \sum_{i=1}^{M_p} E_{p,i}(P_i) + \sum_{j=1}^{M_c} E_{c,j}(O_j, H_j) + \sum_{n=1}^{M_h} E_{h,n}(T_n) \\ = \sum_{i=1}^{M_p} g_i P_i^2 + h_i P_i + k_i + n_i e^{l_i P_i} \\ + \sum_{j=1}^{M_c} \mu_j O_j + \sum_{n=1}^{M_h} v_n T_n \tag{8}$$

where  $E_{p,i}, E_{c,j}, E_{h,n}$ , respectively, represent the emissions of the  $i$ th power-only unit, the  $j$ th CHP unit, and the  $n$ th heat-only unit.  $\mu_j$  represents the emission coefficient of the  $j$ th CHP unit,  $v_n$  represents the emission coefficient of the  $n$ th heat-only unit, and  $M_c, M_h$ , respectively, represent the number of CHP unit and heat-only unit.

### 2.2.2 Constraints

Due to the incorporation of the CHP unit, it is important to ensure that the power of the CHP unit is in the feasible operating zone, in addition to considering the basic constraints of the power-only unit. As can be seen in Fig. 1, points A, B, C, D, E, and F constitute the feasible operating zone for

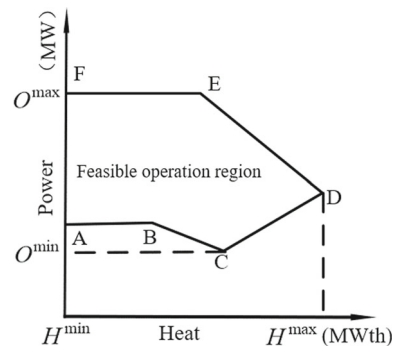


Fig. 1 Feasible operation area of cogeneration unit

the CHP unit. In this operating zone, there is a strong dependence between the heat and power production capacity of the CHP unit, i.e., as the heat production capacity changes, so does its power production capacity, and vice versa. For example, in the BC section, as the electrical output of the CHP unit decreases, its thermal output gradually increases. In the CD section, as the thermal output of the CHP unit rises, its electrical output rises gradually.

The power balance constraint is defined as the actual power generated by the power-only unit and CHP unit equal to the load side power plus the transmission losses between the units.

$$\sum_{i=1}^{M_p} P_i + \sum_{j=1}^{M_c} O_j = Pd + Pl \tag{9}$$

where  $Pd$  represents the electricity demand on the load side. Transmission loss  $Pl$  is shown by Eq. (10).

$$Pl = \sum_{i=1}^{M_p} \sum_{j=1}^{M_p} P_i P_j B_{ij} + \sum_{i=1}^{M_p} \sum_{j=1}^{M_c} P_i O_j B_{ij} + \sum_{i=1}^{M_c} \sum_{j=1}^{M_c} O_i O_j B_{ij} + \sum_{j=1}^{M_c} B_{0j} O_j + \sum_{i=1}^{M_p} B_{0i} P_i + B_{00} \tag{10}$$

where  $B_{ij}$  represents the transmission loss coefficient between the two generating units,  $B_{0i}$  represents the self-loss coefficient of each generating unit, and  $B_{00}$  represents a constant loss coefficient.

The thermal power balance required on the load side is shown in Eq. (11).

$$\sum_{n=1}^{M_h} T_n + \sum_{j=1}^{M_c} H_j = Hd \tag{11}$$

where  $Hd$  represents the total heat demand by the load in the system.

All power-only units, CHP units, and heat-only units have to meet the capacity constraints of the units [33].

$$P_i^{\min} \leq P_i \leq P_i^{\max}, \quad i = 1, 2, \dots, M_p \tag{12}$$

$$T_n^{\min} \leq T_n \leq T_n^{\max}, \quad n = 1, 2, \dots, M_n \tag{13}$$

$$O_j^{\min}(H_j) \leq O_j \leq O_j^{\max}(H_j), \quad j = 1, 2, \dots, M_c \tag{14}$$

$$H_j^{\min}(O_j) \leq H_j \leq H_j^{\max}(O_j), \quad j = 1, 2, \dots, M_c \tag{15}$$

where  $T_n^{\min}$ ,  $T_n^{\max}$  represent the lower and upper limits of the  $n$ th heat-only unit,  $O_j^{\min}$ ,  $O_j^{\max}$  A and B represent the

lower and upper limits of the power production of the  $j$ th CHP unit,  $H_j^{\min}$ ,  $H_j^{\max}$  represent the lower and upper limits of the heat production power of the  $j$ th CHP unit,  $T_n$ ,  $H_j$ ,  $O_j$ , respectively, represent the actual heat production power of the  $n$ th heat-only unit and the actual heat production power and actual power production of the  $j$ th CHP unit.

### 3 Two-Stage Collaborative Multi-objective Differential Evolution Algorithm

#### 3.1 Differential Evolution

Differential evolution (DE) was first proposed by Storn and Price [34]. Because the algorithm has good search ability and robustness, it is now widely used in various practical problems. DE consists of three main processes: mutation, crossover, and selection.

First, the differential operator uses a mutation strategy to generate a set of target vectors  $X_{i,G}^D = (X_{i,G}^1, X_{i,G}^2, X_{i,G}^3, \dots, X_{i,G}^D)$ , where  $D$  represents the dimension of the decision space,  $G$  is the number of iterations,  $i = 1, 2, \dots, N$ , where  $N$  represents the population size. The commonly used mutation strategies are as follows.

$$V_{i,G} = X_{r1,G} + F \cdot (X_{r2,G} - X_{r3,G}) \tag{16}$$

where,  $X_{r1,G}$ ,  $X_{r2,G}$ ,  $X_{r3,G}$  represent individuals randomly selected from the population of the  $G$ th iteration, and these individuals are not equal to each other.  $F$  represents a mutation rate.

Crossover, each individual  $X_{i,G}$  of the  $G$ -generation population and the variant individual  $V_{i,G}$  perform crossover operations between individuals.

$$U_{ij,G} = \begin{cases} V_{ij,G}, & \text{if } rand < CR \text{ or } j = j_{rand} \\ X_{ij,G}, & \text{others} \end{cases} \tag{17}$$

where  $CR$  represents the crossover rate and  $j_{rand}$  represents an integer randomly selected from the decision dimension  $D$ , which guarantees that  $X_{i,G}$  and  $V_{i,G}$  are different in a certain dimension.  $U_{ij,G}$  represents crossover individuals.

Selection, follow the principle of greed to select the next generation of individuals.

$$X_{i,G+1} = \begin{cases} U_{i,G}, & \text{if } f(U_{i,G}) < f(X_{i,G}) \\ X_{i,G}, & \text{others} \end{cases} \tag{18}$$

where  $f(\cdot)$  represents the fitness of the individual and  $X_{i,G+1}$  represents the next generation of individuals.

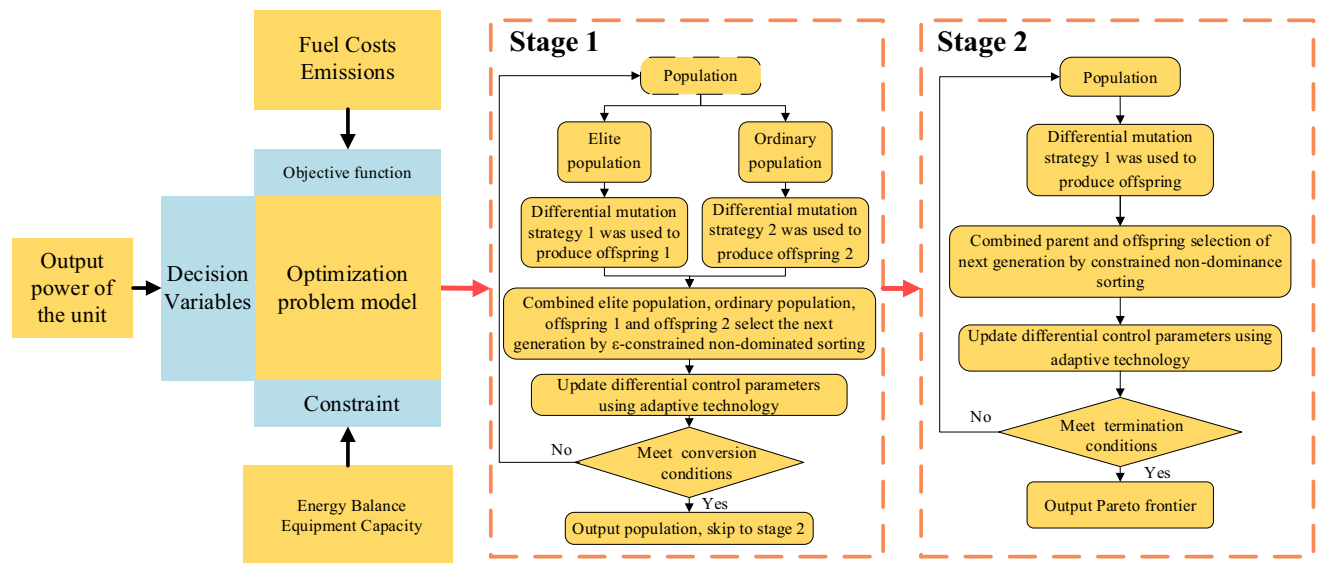


Fig. 2 Framework of TCADEA

### 3.2 Two-Stage Cooperative Multi-objective Evolutionary Differential Algorithm

DE is widely used for solving complex optimization problems. However, DE cannot obtain a set of optimal PF when solving multi-constraint and multi-objective problems. For this reason, a two-stage cooperative multi-objective differential algorithm (TCADEA) is proposed in this paper to obtain the PF for multi-objective and multi-constrained CHPEED problems. TCADEA uses a two-stage framework. The first stage uses different mutation strategies to update elite population and ordinary population and uses  $\varepsilon$ -constrained non-dominated sorting to ensure that populations obtain a large number of feasible solutions. The second stage ensures that the population finds more good individuals in the feasible domain by means of the differential operator and constrained non-dominated sorting. In addition, adaptive techniques are used to update the differential control parameters throughout the evolutionary process. The overall framework is shown in Fig. 2.

#### 3.2.1 The First Stage

The first stage aims to find a large number of feasible solution individuals in the target space. Therefore, the use of a dual-population framework and  $\varepsilon$ -constrained non-dominated sorting in this stage is to ensure that the population can obtain high-quality solution quickly.

##### (a) Dual-population framework

Elite population contain high-quality individuals in the population, and elite individuals undergo evolution to provide

more high-quality solutions to the population. Therefore, the elite population uses the following mutation strategy to generate offspring.

$$X_{i,G} = X_{i,G} + F_G \cdot (X_{r1,G} - X_{r2,G}) \quad (19)$$

where  $X_{i,G}$ ,  $X_{r1,G}$ ,  $X_{r2,G}$  represents the different individuals in the elite population.  $F_G$  represents the mutation rate.

The ordinary population contains secondary individuals of the population that need to be guided by elite individuals to obtain better offspring. Its mutation strategy is as follows.

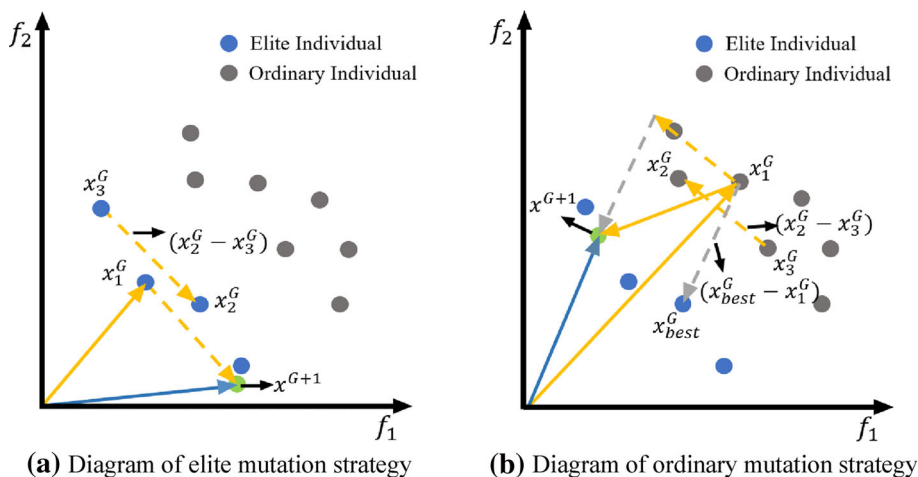
$$X_{i,G} = X_{i,G} + F_G \cdot (X_{best,G} - X_{i,G}) + F_{max} \cdot (X_{r1,G} - X_{r2,G}) \quad (20)$$

where  $X_{i,G}$ ,  $X_{r1,G}$ ,  $X_{r2,G}$  represent the different individuals in the ordinary population.  $X_{best,G}$  represents elite individual.  $F_{max}$  represents the maximum mutation rate.

Figure 3 shows the effects of the two mutation strategies on the two populations. In Fig. 3a, elite individual  $x_1^G$  combined with other elite individuals  $x_2^G$  and  $x_3^G$  generates more elite individuals through Eq. (19). In Fig. 3b, ordinary individual  $x_1^G$  combined with other ordinary individuals  $x_2^G$  and  $x_3^G$  under the guidance of elite individual  $x_{best}^G$  through Eq. (20) to produce individuals with better target value, which can provide more solutions to the elite population in the process of selecting the next generation of individuals.

In order to dynamically adjust the mutation rate  $F$  and crossover rate  $CR$  in the differential operator, an adaptive parameter technique is proposed in this paper. It is shown as follows:

Fig. 3 Mutation strategy diagram



$$F_G = F_{\max} \cdot (1 - gen) \tag{21}$$

individual B is placed in the last level. Through  $\varepsilon$ -constrained non-dominance ranking, the population is able to obtain valid information among infeasible individuals to enable the population to produce more high-quality solutions.

$$\varepsilon(G) = \begin{cases} \Phi_{\max}^G & \text{if } G = 0 \\ (1 - \psi) * \varepsilon(G - 1) & \text{if } Pf^G < \Upsilon, (1 - \psi) * \varepsilon(G - 1) > \Phi_{\min}^G \\ rand() * (\Phi_{\max}^G - \Phi_{\min}^G) + \Phi_{\min}^G & \text{if } Pf^G < \Upsilon, (1 - \psi) * \varepsilon(G - 1) < \Phi_{\min}^G \\ 0 & \text{if } Pf^G \geq \Upsilon \end{cases} \tag{23}$$

$$CR_G = \begin{cases} 0.8 & \text{if } G < \partial \cdot \maxgen \\ 0.2 & \text{others} \end{cases} \tag{22}$$

where  $F_{\max}$  represents the maximum mutation rate and  $gen$  represents the ratio of the number of iterations  $G$  to the maximum number of iterations  $\maxgen$ .

(b)  $\varepsilon$ -Constrained non-dominated sorting

To solve the multi-objective and multi-constraint conditions in the economic emission dispatch problem, an  $\varepsilon$ -constrained non-dominated sorting is proposed in this paper. The purpose of this method is to set a constraint violation threshold  $\varepsilon$  to select individuals in the population with small target and constraint violation values, and to produce offspring with good target values by combining these individuals with feasible individuals in the population where  $\varepsilon$ -constrained non-dominated sorting and threshold  $\varepsilon$  are shown in Fig. 4 and Eq. (21), respectively.

Figure 4 shows that the population selects individuals by  $\varepsilon$ -constrained non-dominated sorting. Individuals B, C, and D are infeasible individuals in the Figure, where individuals C and D possess good target values. Since the constraint violation values of individuals C and D are less than  $\varepsilon$  and the constraint violation value of individual B is greater than  $\varepsilon$ , individuals C and D are selected into the second level and

where  $\Phi_{\max}^G$ ,  $\Phi_{\min}^G$ , respectively, represent the maximum and minimum values of contemporary constraint violations,  $Pf^G$  represents the ratio of feasible solutions in the contemporary population.  $\Upsilon$  represents the search preference for controlling feasible and infeasible regions.  $\psi$  represents the reduction in the value of  $Pf^G < \Upsilon$  when  $\varepsilon$  is controlled. When  $(1 - \psi) * \varepsilon(G - 1) < \Phi_{\min}^G$ , it is necessary to quantify the channel individuals to ensure that the population is moving in the optimal direction, and then the value of  $\varepsilon$  is reset to  $rand() \cdot (\Phi_{\max}^G - \Phi_{\min}^G) + \Phi_{\min}^G$ .

3.2.2 The Second Stage

When a large number of feasible solutions are found in the first stage, we combined the elite population with the ordinary population and ensured that the population could obtain more feasible solutions by updating the population using the adaptive difference operator and selecting the next generation according to the CDP. As shown in Fig. 5, when entering the second stage, most of the solutions in the population lie within the feasible region and the target values do not differ much. Therefore, there is no need to divide the population into two populations, and it is sufficient to generate offspring by adaptive differential operators. The next generation is also

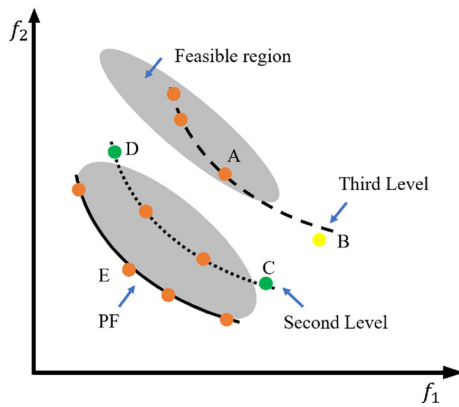


Fig. 4  $\varepsilon$ -constrained non-dominated sorting

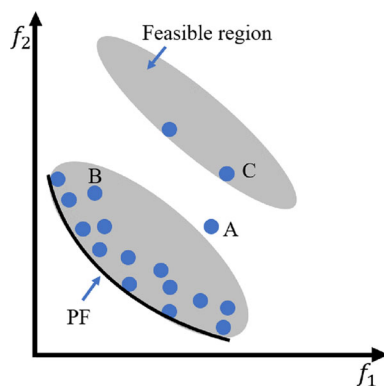


Fig. 5 Stage 2

selected according to CDP, i.e., the feasibility of both individuals is checked first. If both individuals are feasible, the individuals are selected based on Pareto dominance. In Fig. 5, A is an infeasible individual and B and C are feasible individuals. According to the CDP, A is compared with B and C to eliminate individual A, and B is compared with C. Based on Pareto dominance, individual B wins.

When the population enters the second stage, the following criteria need to be met:

1. The overall constraint violation value  $A_{oc}$  in the first stage varies less than  $V_e$  at  $n$  generations apart

$$A_{oc} = \frac{|\text{sum}(\varepsilon_G) - \text{sum}(\varepsilon_{G-n})|}{\text{sum}(\varepsilon_G)} < V_e \quad (24)$$

2. The contemporary constraint violation average  $A_{ve}$  is less than  $C_{va}$

$$A_{ve} = \frac{\text{sum}(\varepsilon_G)}{N} < C_{va} \quad (25)$$

Here  $V_e$  and  $C_{va}$  are set to  $10^{-3}$  and  $10^{-4}$ , respectively.  $\varepsilon_G$  represents the constraint violation value for each individual in the  $G$ -th generation. Condition 1 determines whether the population reaches the neighborhood of the feasible region. Condition 2 determines the proportion of feasible solutions in the population.

### 3.2.3 Algorithm Steps

Through the above analysis of the algorithm proposed in this article, we can get its specific steps:

**Step1:** The initial population  $P$  is generated according to the power interval of each unit. Set the population size to  $N$ , the maximum number of iterations to  $\text{maxgen}$ , and the number of iterations counter to  $m = 0$ .

**Step2:** Determine whether  $m$  is greater than or equal to  $\text{maxgen}$ . If it holds, output PF. Otherwise, execute the following steps.

**Step3:** Determine whether Eqs. (24) and (25) are valid. If it holds, skip to step 7. Otherwise, perform step 4.

**Step4:** The population is divided into elite population P1 and ordinary population P2 according to the non-dominated level and crowding; the elite population P1 uses Eq. (19) to generate offspring, and the ordinary population uses Eq. (20) to generate offspring and calculate the target value for each individual.

**Step5:** Obtaining next-generation populations by  $\varepsilon$ -constrained non-dominated sorting.

**Step6:** Update  $A_{oc}$  and  $A_{ve}$  with  $m = m + 1$  and return to step 2.

**Step7:** Determine whether  $m$  is greater than or equal to  $\text{maxgen}$ . If it holds, output PF. If not, execute the following steps.

**Step8:** The elite population P1 and ordinary population P2 are combined into one population and the offspring are generated according to Eq. (19).

**Step9:** Get the next generation according to CDP.

**Step10:** Update  $m = m + 1$  and return to step 7.

## 4 Experimental Results and Analysis

In this section, firstly, the effectiveness of the algorithm proposed in this paper is verified using a test function. Secondly, to test the feasibility of the algorithm in real-world problems, we use three standard cases as well as a real case to verify it. Case 1 includes one power-only unit, one heat-only unit and three CHP units. Case 2 includes ten pure electric units with valve point effects and transmission loss. Case 3 includes four power-only units, two CHP units, and one heat-only unit, with valve point effects and transmission loss. NSGA-II,



**Table 1** Various index values of different algorithms in the test function

Problem	MODE, NSGA-II, TOP, TCADEA							
	IGD				HV			
CF1	5.2000e−1 (2.02e−1) −	6.1041e−2 (5.54e−3) −	2.1178e−2 (4.46e−3) −	<b>9.1009e−3</b> <b>(1.93e−3)</b>	1.9105e−1 (1.06e−1) −	4.9064e−1 (7.05e−3) −	5.4082e−1 (5.22e−3) −	<b>5.5506e−1</b> <b>(2.32e−3)</b>
CF2	5.1439e−2 (8.90e−3) −	7.3076e−2 (2.42e−2) −	5.9493e−2 (8.20e−2) −	<b>2.8551e−2</b> <b>(9.86e−3)</b>	5.9340e−1 (2.00e−2) −	5.8253e−1 (3.81e−2) −	6.1282e−1 (3.62e−2) −	<b>6.4601e−1</b> <b>(1.09e−2)</b>
CF3	9.7570e−1 (2.01e−1) −	<b>2.9556e−1</b> <b>(6.25e−2)</b> =	6.9695e−1 (9.87e−2) −	3.0336e−1 (1.23e−1)	0.0000e + 0 (0.00e + 0) −	1.3307e−1 (4.87e−2) =	7.9249e−4 (2.28e−3) −	<b>1.1102e−1</b> <b>(4.34e−2)</b>
CF4	1.7262e−1 (3.66e−2) −	1.3749e−1 (5.65e−2) −	9.7940e−2 (2.98e−2) −	<b>9.1551e−2</b> <b>(3.83e−2)</b>	3.0673e−1 (3.31e−2) −	3.7536e−1 (5.28e−2) −	3.9903e−1 (3.22e−2) −	<b>4.2317e−1</b> <b>(3.20e−2)</b>
CF5	2.3632e + 0 (5.04e−1) −	3.2527e−1 (1.50e−1) =	7.1613e−1 (2.29e−1) −	<b>2.7623e−1</b> <b>(8.21e−2)</b>	0.0000e + 0 (0.00e + 0) −	2.3801e−1 (6.06e−2) =	2.9298e−2 (4.62e−2) −	<b>2.4056e−1</b> <b>(7.82e−2)</b>
CF6	<b>7.5651e−2</b> <b>(3.02e−2)</b> +	1.1344e−1 (4.78e−2) =	8.6235e−2 (3.04e−2) =	1.0817e−1 (4.73e−2)	6.3515e−1 (1.20e−2) =	6.0762e−1 (2.53e−2) −	6.1748e−1 (1.54e−2) −	6.3143e−1 (2.26e−2)
CF7	4.8150e−1 (1.89e−1) −	3.2767e−1 (1.64e−1) −	7.1801e−1 (3.08e−1) −	<b>2.1428e−1</b> <b>(7.58e−2)</b>	1.7725e−1 (1.34e−1) −	4.0101e−1 (1.15e−1) =	8.5869e−2 (1.11e−1) −	<b>4.3447e−1</b> <b>(8.49e−2)</b>
± / =	1/6/0	0/4/3	0/6/1		0/6/1	0/4/3	0/7/0	

TOP, and MODE are compared with the proposed algorithm with a population size of 100 and a maximum number of iterations of 200, where the maximum number of iterations for the real case is 1000. The proposed algorithm was implemented in Matlab 2018b and executed on a PC equipped with an Intel Core i5 processor with 4 GB of memory.

### 4.1 Algorithm Improvement Effectiveness Test

Considering that CEED and CHPEED are constrained multi-objective minimization problems, we use the constrained multi-objective model of reference [35]. TCADEA was compared with MODE, NSGA2, and TOP [36] on the constrained multi-objective test set CF.

In order to analyze the performance of the TCADEA algorithm more easily, the inverse generation distance (IGD) and the hypervolume (HV) will be used for qualitative evaluation. IGD and HV can simultaneously reflect the convergence and diversity of the algorithm. +, − and ≈ A, B and C, respectively, represent that other algorithms are better, TCADEA is better, and there is no significant difference between them.

As seen in Table 1, the TCADEA algorithm obtains significantly better results on the seven test problems and the proposed algorithm has an IGD close to 0 and the HV value is the largest, which shows that the proposed algorithm maintains population convergence while ensuring

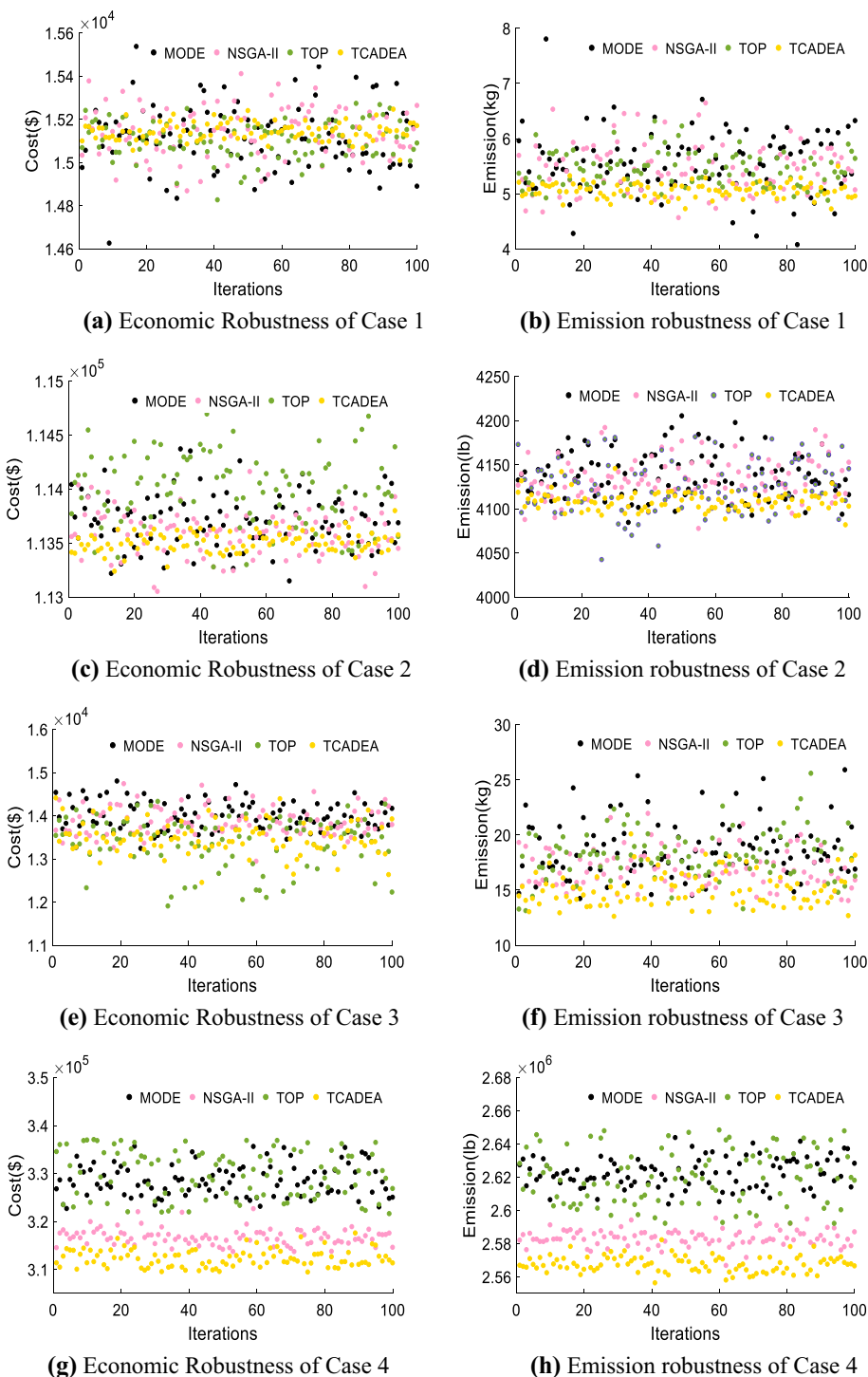
better population distributivity. This is because the constraint processing technique adopted in this paper is able to handle the constraints in the constraint problem very well. Meanwhile, the adopted dual-population framework can improve the convergence of populations by adopting different mutation strategies according to the characteristics of different populations. The bolded black font in the tables all represent excellent values in a given problem in this paper.

Due to the stochastic character of intelligent optimization algorithms, the results of a single run do not prove that the algorithm can solve a problem well. Therefore, to demonstrate the robustness of TCADEA for economic emission dispatch problems, we will perform 100 experiments for each of the different cases and compare them with MODE, NSGA-II, and TOP. It can be seen from Fig. 6 that the distribution of solutions obtained by the TCADEA algorithm is concentrated compared to MODE, NSGA-II, and TOP, which shows the good robustness of the TCADEA algorithm in the economic emission dispatch problem.

### 4.2 Case 1

This case has a total of five units, one power-only unit, three CHP units and one heat-only unit. The electrical load demand is 300 MW, and the heat load demand is 150 MWth. The model parameters can be found in [27]. To demonstrate more

**Fig. 6** Robustness distribution diagram of different cases



intuitively the distributivity of the solutions solved by the algorithm, we compare the optimal PFs obtained at the end of the run for NSGA-II, MODE, TOP, and TCADEA, as shown in Fig. 7.

It can be seen from Fig. 7 that TCADEA can obtain a uniform and convergent PF in the CHPEED problem. Compared to NSGA-II, MODE, and TOP, TCADEA contains a more extensive solution and offers a lot more options. Figure 7

demonstrates that TCADEA has a good ability to optimize this problem. It is also evident that fuel costs and emissions are two conflicting goals. As the fuel cost increases, it leads to a decrease in emissions. Therefore, to facilitate the comparison between TCADEA and other algorithms, we take the best compromise solution from the optimal solution set. The best compromise solution is the one that is the most intermediate solution in the PF, i.e., by ranking the PFs according

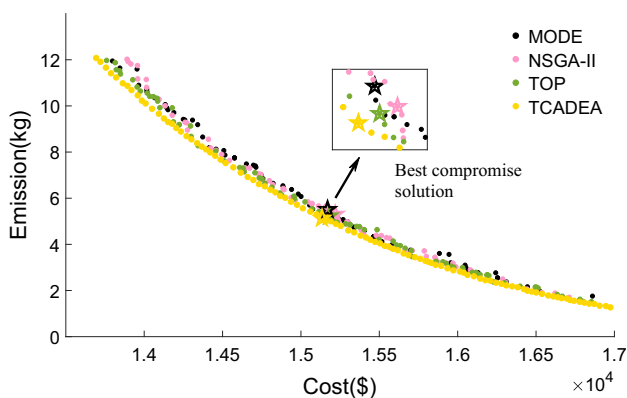


Fig. 7 PF of the four test algorithms in Case 1

to their economic objectives to obtain the ranking order, and then selecting the individual with the middle ranking number as the best compromise solution to the optimization problem. The best compromise solution is indicated by an asterisk in Fig. 7.

Table 2 shows the best compromise solutions for NSGA-II, TOP, IDBEA, BCS1, MODE, and TCADEA. By analyzing the model parameters in [27], we can know that the impact of power-only units on emissions is high and the impact of electrical power of CHP units on fuel costs is high. In Table 2, the output of the power-only unit of TCADEA is 85.9 MW, which is the smallest among several tested algorithms, and the total electrical power of the CHP unit is also the smallest. As a result, the fuel cost of TCADEA is reduced by \$84, \$55, \$57, \$151.3, and \$35, and the emissions are reduced by 0.17 kg, 0.1 kg, 0.07 kg, 0.27 kg, and 0.37 kg, respectively. Figure 8 shows the unit output power for the economic optimal solution (ECOS) and the emission optimal solution (EMOS) obtained by the TOP and TCADEA algorithms in Case 1. From the analysis of Table 2, it is clear that the impact of power-only units on emissions is high and the impact of electrical power of CHP units on fuel costs is high. Among the three CHP units, the power increase of unit 2 has the

greatest impact on fuel cost. In Fig. 8a, the electric power of TCADEA’s CHP unit is 6 MW less than TOP, so TCADEA can obtain lower fuel cost. In Fig. 8b, the output power of TCADEA’s power-only unit is 6.7 MW less than TOP, so TCADEA gets less emissions.

The convergence and diversity of the obtained solution sets are verified using the metrics in reference [37]. Some of the evaluation metrics in multi-objective optimization algorithms require reference solution sets, but in practical problems there are often no reference solution sets. Therefore, to facilitate the comparison of the results in the paper, three metrics are selected to compare the convergence and diversity of the algorithms, namely hypervolume (HV), spacing metric (SM), diversity metric (DM). The HV is used to evaluate the convergence of the algorithm. The SM and the DM evaluate the uniformity and extensiveness of the solution set, respectively, and the combination of both can be used to evaluate the diversity of the algorithm.

In Table 3, the HV of TCADEA is the largest, and SM and DM are close to zero with regard to the other algorithms, which shows that the TCADEA algorithm can obtain better PF and has good convergence and diversity in Case 1.

### 4.3 Case 2

In order to verify the broadness of the proposed algorithm in practical applications, the algorithm is applied to the CEED problem. The case has a total of ten power-only units, with valve point effects and transmission loss. The electrical load demand is 2000 MW, and the model parameters are available in Reference [38].

The analysis of the model parameters for this Case shows that unit 9 has the greatest impact on the fuel cost and emissions of CEED. In Table 4, the output power of unit 9 obtained by TCADEA is the smallest compared to NSGA-II, TOP, MODE, PDE, and GSA, with the result of 428.158 MW. As a result, TCADEA’s fuel costs and emissions were reduced

Table 2 Results obtained in Case 1 for different testing algorithms

Outputs	NSGA-II	TOP	IDBEA [24]	BCS1 [25]	MODE	TCADEA
P1 (MW)	87.3	86.8	87.1	88.2	89.6	85.9
O1 (MW)	78.7	65.6	95.5	94.1	66.5	79.9
H1 (MWth)	59.8	80.4	17.3	33.2	88.1	88.5
O2	42.3	49.8	100.2	85.1	39.8	30.4
H2	41.4	30.6	61.4	72.6	44.5	19.7
O3	91.7	98	41	29.5	104.1	103.5
H3	7.7	7.9	0.2	12.3	1.4	0
T1	41.2	31.1	49	35.7	16	41.8
Cost (\$)	15,219	15,180	15,182	15,286.3	15,170	15,135
Emission (kg)	5.3	5.23	5.2	5.4	5.50	5.13

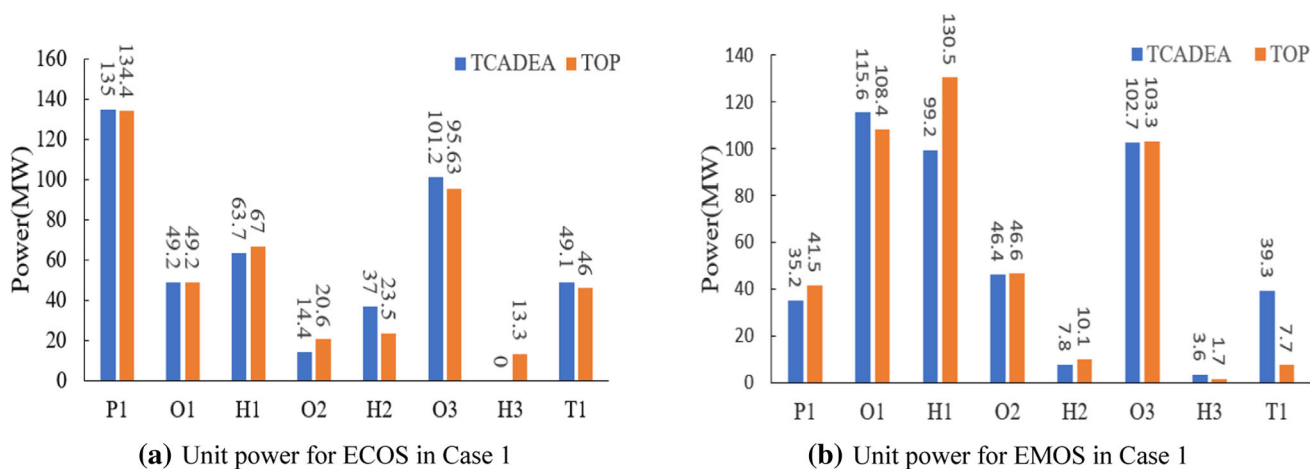


Fig. 8 Unit power of ECOS and EMOS in Case 1 for TCADEA and TOP

Table 3 Various index values of different test algorithms in Case 1

Criteria	MODE	NSGA-II	TOP	TCADEA
HV	0.6224	0.6290	0.6172	0.6293
SM	0.0183	0.0113	0.0115	0.0057
DM	0.5376	0.6374	0.5652	0.5338

Table 4 Results of different test algorithms in Case 2

Outputs (MW)	NSGA-II	TOP	MODE	PDE [38]	GSA [39]	TCADEA
P1	52.837	54.205	54.054	54.985	54.999	54.361
P2	79.547	74.223	73.092	79.380	79.958	78.855
P3	80.671	89.616	101.3958	83.984	79.434	91.585
P4	95.923	87.255	83.276	86.594	85.0	82.272
P5	142.085	149.86	147.126	144.438	142.106	145.211
P6	174.285	162.964	164.2481	165.775	166.567	165.276
P7	285.961	287	294.71	283.212	292.874	298.111
P8	298.586	294.986	300.908	312.770	313.238	298.88183
P9	432.412	443.001	420.004	440.130	441.177	428.251
P10	441.335	441.062	445.010	432.678	428.630	440.291
Ploss (MW)	83.6	84.2	83.8	83.9	83.98	83.1
Cost (\$)	113,685.3	113,591.4	113,610.8	113,517.3	113,492.8	113,485.6
Emission (lb)	4112.2	4118.8	4127.3	4111.4	4111.4	4107.4

by \$199.7, \$105.8, \$125.2, \$31.7, \$7.2 and 4.8 lb, 11.4 lb, 19.9 lb, 4 lb, 4 lb, respectively. It is worth noting that the transmission loss of TCADEA is the smallest because the transmission loss is related to the output power of the unit, and the output power of each unit of the proposed algorithm is the smallest sum. In summary, TCADEA is more effective in energy saving and emission reduction in the CEED problem.

Figure 9 shows the PFs obtained by MODE, NSGA-II, TOP, and TCADEA for the CEED problem. In Fig. 9, the

PF of TCADEA possesses good extensiveness and uniformity. Compared with NSGA-II, MODE, and TOP, most of the solutions of TCADEA are better than all three, which can more intuitively show that TCADEA has good superiority in the CEED problem.

From Table 5, it can be seen that TCADEA is \$333, \$136, and \$377 less than MODE, NSGA-II, and TOP, respectively, in the fuel cost optimum case. In the emission optimal case, TCADEA emits 22.6 lb, 12.6 lb, and 15.8 lb less than MODE, NSGA-II, and TOP, respectively. This shows that

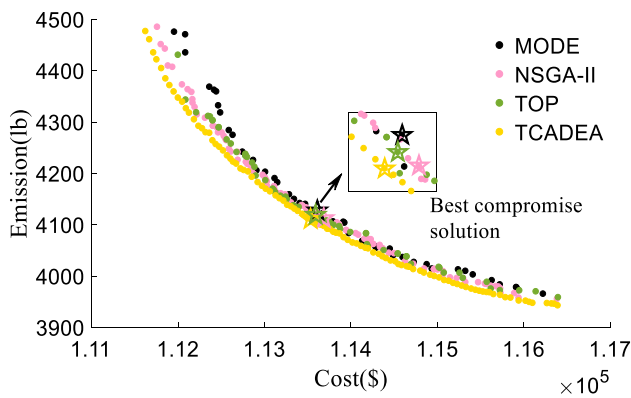


Fig. 9 The PFs of the four test algorithms in Case 2

the TCADEA algorithm provides a more extensive solution for decision makers.

Figure 10 shows the unit output power of ECOS and EMOS obtained by TOP and TCADEA algorithms in Case 2. The analysis of the model parameters shows that the squared term coefficients in the fuel cost functions of units 7–10 are the smallest among all units, so the amount of their changes has the least effect on the fuel cost functions when the output power of the units increases. The quadratic term coefficients in the emission functions of units 1–4 are – 80 times the primary term coefficients, while units 7–10 are – 110 times, which indicates that the changes in emissions are mainly caused by units 7–10. In Fig. 10a, the output of unit 7–10 in TCADEA is larger than that of TOP, so it has a smaller change in fuel cost. In Fig. 10b, the emission of unit 7–10 in TCADEA is 2086.7 lb, and the emission of unit 7–10 in TOP is 2102.1 lb, so it is obvious that the emission of TCADEA is less.

In Table 6, TCADEA has a larger HV and smaller SM and DM compared to NSGA-II, MODE and TOP. This shows that the TCADEA algorithm is able to obtain better PF and the diversity of the solutions obtained.

### 4.4 Case 3

To better demonstrate the practicality and validity of the method in this paper, a more complex test system was introduced. This test system contains four power-only units (units

1–4), two CHP units (units 5–6), and one heat-only unit (unit 7). The system includes valve point effect and transmission loss. The electrical load demand is 600 MW, and the heat load demand is 150 MWth. The model parameters can be found in [27].

In Fig. 11, the solutions of TCADEA are more widely distributed and have more solutions compared to NSGA-II, MODE, and TOP. In addition, the optimal PF of the four algorithms shows that the performance of the TCADEA solution is better in most cases. This indicates that the constraint processing technique of the proposed algorithm is able to solve the constraints in the CHPEED problem to provide more solutions for the population.

In Table 7, the HV of TCADEA is the largest, and SM and DM are close to zero compared to the other algorithms, which shows the good convergence and diversity of the TCADEA algorithm in Case 3.

Table 8 shows the best compromise solution, ECOS and EMOS for the four tested algorithms. Based on the model parameters in [27], we can see that the impact of power-only units on emissions is larger and the impact of CHP units on fuel costs is larger. From Table 8, it is concluded that the total output power of the power-only units is approximately equal for each algorithm in the best compromise solution, while the total output power of the CHP units is the smallest for TCADEA. As a result, the fuel cost and emissions of TCADEA are reduced by \$108.7, \$220.4, \$55.6, and 1.2 kg, 0.4 kg, 1.2 kg compared to NSGA-II, MODE, and TOP, respectively. The optimal fuel cost and optimal emissions of TCADEA are also minimized under both ECOS and EMOS.

Figure 12 gives the transmission loss for the different test algorithms under the three different solutions. It can be seen from Eq. (10) that the transmission loss of the system is related to the electrical power of each power producing unit. In Table 7, the total electrical power obtained by TCADEA is the smallest in the three cases. Therefore, the transmission loss of TCADEA under the best compromise solution is reduced by 1.9 MW, 0.5 MW, and 0.9 MW compared to NSGA-II, MODE, and TOP. The transmission loss of TCADEA under ECOS is reduced by 0.4 MW, 1.1 MW, and 9.1 MW compared to NSGA-II, MODE, and TOP. The transmission loss of TCADEA under EMOS is reduced by

Table 5 Multiple solutions of the test algorithm in Case 2

Methods	Best fuel cost		Best emission		Best compromise	
	Cost (\$)	Emission (lb)	Cost (\$)	Emission (lb)	Cost (\$)	Emission (lb)
MODE	111,956	4475.3	116,224	3965.1	113,635	4138.7
NSGA-II	111,759	4484.9	116,386	3955.1	113,994	4128.4
TOP	112,000	4430.4	116,397	3958.3	113,567	4104.5
TCADEA	<b>111,623</b>	4476.5	116,394	<b>3942.5</b>	<b>113,497</b>	<b>4101.4</b>

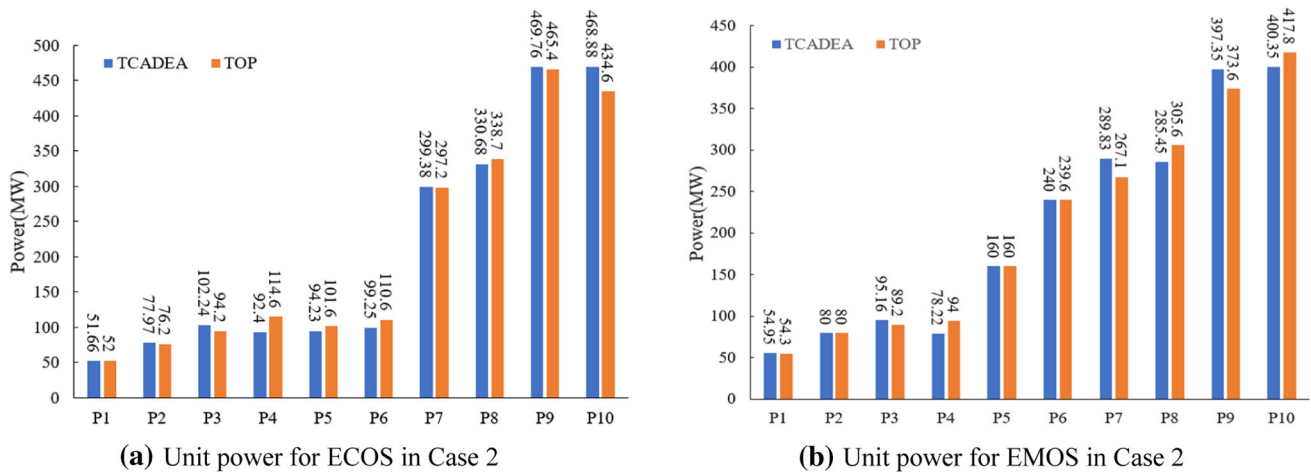


Fig. 10 Unit power of ECOS and EMOS in Case 2 for TCADEA and TOP

Table 6 Various index values of different test algorithms in Case 2

Criteria	MODE	NSGA-II	TOP	TCADEA
HV	0.8200	0.6974	0.6959	0.7104
SM	0.0158	0.0167	0.0167	0.0077
DM	0.5108	0.5410	0.7897	0.5104

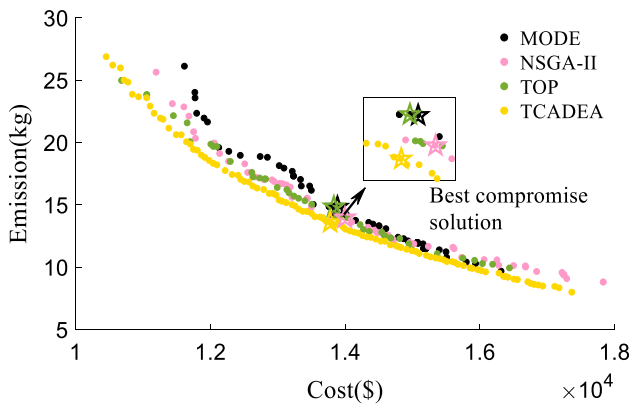


Fig. 11 The PFs of the four test algorithms in Case 3

Table 7 Various index values of different test algorithms in Case 3

Criteria	MODE	NSGA-II	TOP	TCADEA
HV	0.6506	0.6299	0.5934	0.6672
SM	0.0206	0.0153	0.0203	0.0079
DM	0.9171	0.8884	0.9203	0.5644

2.3 MW, 11 MW, and 0.6 MW compared to NSGA-II, MODE, and TOP.

Figure 13 shows the unit output power of ECOS and EMOS obtained by TOP and TCADEA algorithms in Case 3. The analysis of the model parameters shows that the fuel cost

of the power-only unit is much lower than the other units and the emissions of the CHP unit are much lower than the other units for the same amount of electricity generated. Therefore, the fuel cost and emissions are reduced by increasing the power of the power-only unit and CHP unit. In Fig. 13a, the total power of the power-only unit of the TCADEA algorithm is greater than the total power of the power-only unit of the TOP algorithm, and thus TCADEA can obtain a solution with lower fuel cost. In Fig. 13b, the total power of the CHP units of the TCADEA algorithm is greater than the total power of the CHP units of the TOP algorithm, and thus TCADEA can obtain a solution with lower emissions.

### 4.5 Case 4

The dispatch cycle for this case is one day. The daily load data graph is shown in Fig. 14. The system contains eight power-only units, two CHP units and one heat-only unit, and valve point effects and transmission loss are taken into account.

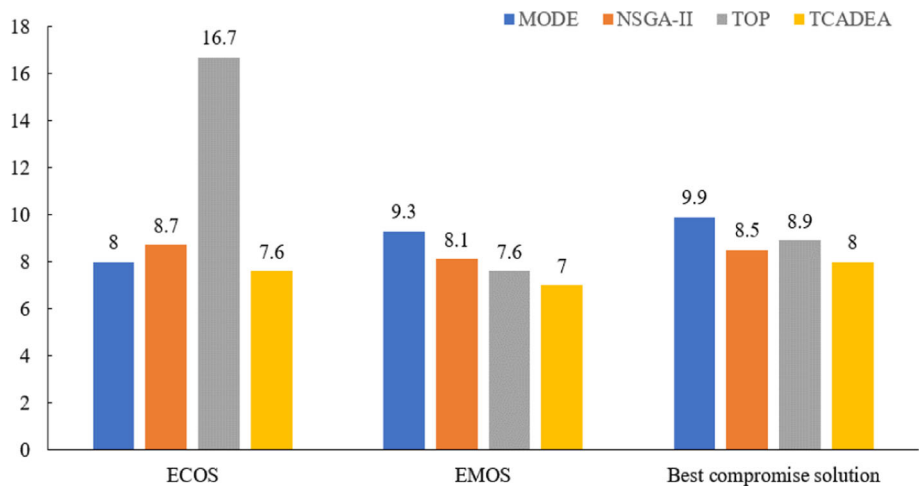
Figure 15 shows the PF obtained by MODE, NSGA-II, TOP, and TCADEA on the daily dispatch problem. In Fig. 15, the PF of TCADEA possesses good extensiveness and convergence. Compared to MODE, NSGA-II and TOP, most of TCADEA’s solutions are close to the coordinate origin, which is a more intuitive indication that TCADEA is able to obtain high-quality solutions with small economy and emissions on daily dispatch.

The best compromise solutions for MODE, NSGA-II, TOP, and TCADEA are given in Table 9. In Table 9,

**Table 8** Results of different test algorithms in Case 3

Outputs	Best compromise solution				Best cost solution				Best emission solution			
	MODE	NSGAI	TOP	TCADEA	MODE	NSGAI	TOP	TCADEA	MODE	NSGAI	TOP	TCADEA
P1 (MW)	54.8	53.3	66.1	51.1	37.5	52.5	66.1	72	29.9	35.5	17	42
P2	60.1	62.6	56.8	78.4	103.3	82.4	106.4	101.3	61.2	60.5	53.8	52.8
P3	110	103.9	98.6	87.4	76.1	139.2	114.7	140	65.4	67.7	93.8	43
P4	119.4	116.4	134.7	114.9	219	179.3	167.4	158.7	116	99.4	102.3	104
O1 (MW)	186.5	215.5	189.7	232	126.5	104.8	111	94	234.1	224.8	242.2	244.9
H1 (MWth)	23.3	45.2	28.2	2.2	78.8	52.2	2.8	32.1	12.1	104.7	11.5	3
O2	77.2	56	72.8	43.8	46.9	49.9	42	41	103.3	120.6	99.8	120.3
H2	47.3	63.2	89.8	69.1	23.4	47.8	72.8	66.7	75.3	27.1	53.5	67.1
T1	79.4	41.6	32	78.7	47.8	50	74.4	51.2	62.6	18.2	85	79.9
Cost (\$)	13,885.3	13,997.7	13,832.5	13,776.6	11,618	11,198.3	10,684.3	10,457.2	16,320.1	17,836.8	16,444.3	17,369.5
Emission (kg)	14.8	14	14.8	13.6	26.1	25.6	24.9	26.8	9.6	8.8	9.9	7.8

**Fig. 12** Transmission loss of different solutions of different test algorithms in Case 3



TCADEA reduces  $\$0.034 \times 10^6$ ,  $\$0.008 \times 10^6$ ,  $\$0.07 \times 10^6$  and  $113 \times 10^5$  lb,  $102 \times 10^5$  lb,  $155 \times 10^5$  lb in terms of fuel cost and emissions compared to MODE, NSGA-II, and TOP, respectively. This indicates that the TCADEA algorithm can provide decision makers with better solutions for the target values.

Figure 16 shows the fuel costs and emissions for each moment of the day for the best compromise solution of TCADEA and TOP. In Fig. 16, the fuel cost and emissions of TCADEA are smaller than those of TOP at almost every moment. This indicates that TCADEA also performs better than TOP in real Cases.

The model parameters for this case show that the impact in terms of fuel cost is greatest for units 1–2, followed by units

3–4, and least for units 5–8. As a result, in Fig. 17a, units 5–8 are operating at full load power between 4:00–22:00. Units 3–4 are also operating at full load power during the peak electricity consumption period of 8:00–15:00. In terms of emissions impact, CHP units emit much less than other units when generating the same amount of electricity. Therefore, the generation power of the CHP units is maintained near the maximum power production during 00:00–24:00. In Fig. 17b, the heating power of the heat-only unit has been maintained at about 300 MW, which is much higher than the heat energy provided by the CHP unit. This is because the fuel cost function of the CHP unit takes into account not only the heat production power but also the power generation

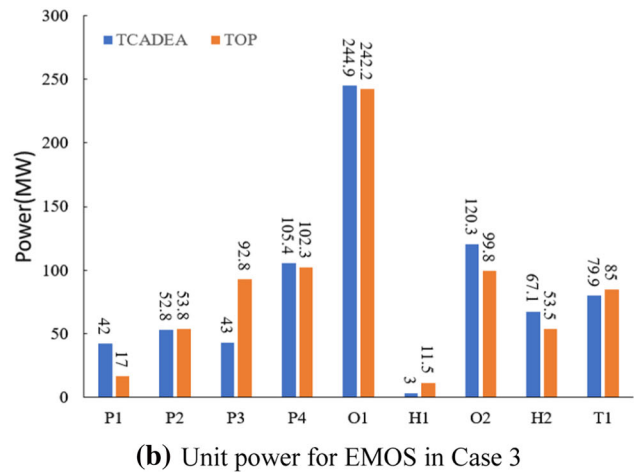
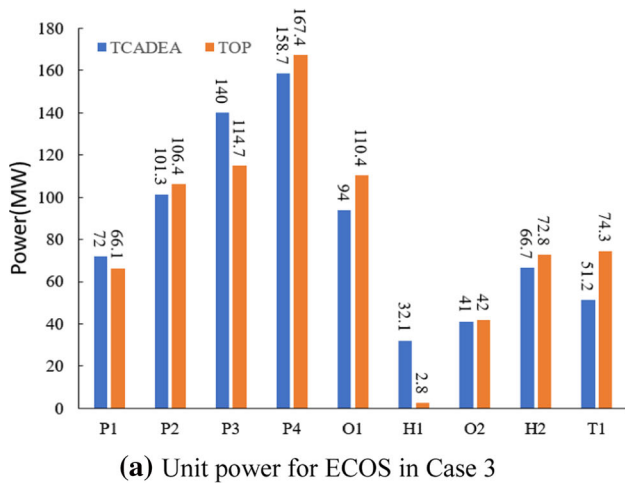


Fig. 13 Unit power of ECOS and EMOS in Case 3 for TCADA and TOP

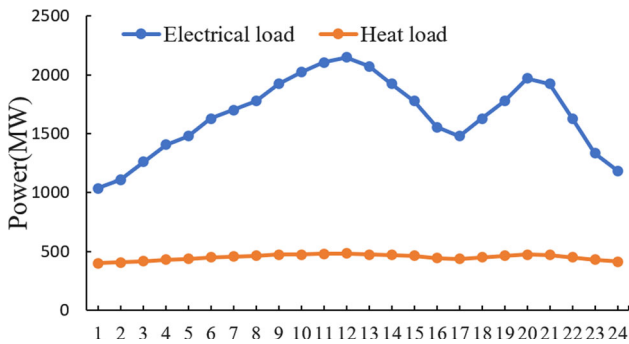


Fig. 14 Daily load data

Table 9 Best compromise solutions for the four tested algorithms

	MODE	NSGA-II	TOP	TCADA
Cost ( $\times 10^6$ \$)	2.687	2.661	2.723	2.653
Emission ( $\times 10^5$ lb)	2.768	2.657	2.805	2.655

### 5 Conclusion

To ensure that lower fuel costs and emissions can be obtained in the economic emission dispatch of power systems, a two-stage cooperative adaptive differential evolutionary algorithm is proposed in this paper. In the first stage, the population is divided into elite populations and ordinary population and combined with two variation strategies and  $\epsilon$ -constrained non-dominated sorting in order to obtain more solutions. In the second stage, more feasible solutions are generated through CDP and Pareto advantage, which gives decision makers more options to choose.

The modeling of the economic emission dispatch problem for power systems takes into account valve point effects and transmission losses. By testing the proposed algorithm for CEED and CHPEED, the results effectively demonstrate the good practicality and generality of TCADA for this class of problems. For the CEED problem, the transmission loss of the best compromise solution of TCADA in Case 2 is reduced by 0.5 MW, 1.1 MW, and 0.7 MW compared to NSGA-II, MODE, and TOP. For the CHPEED problem, TCADA’s fuel cost and emissions in Case 3 are reduced by \$108.7, \$220.4, \$55.6, and 1.2 kg, 0.4 kg, 1.2 kg compared to NSGA-II, MODE, and TOP, respectively. The actual case results show that the TCADA algorithm reduces  $\$0.034 \times 10^6$ ,  $\$0.008 \times 10^6$ ,  $\$0.07 \times 10^6$  and  $113 \times 10^5$  lb,  $102 \times 10^5$  lb,  $155 \times 10^5$  lb in fuel cost and emissions compared to

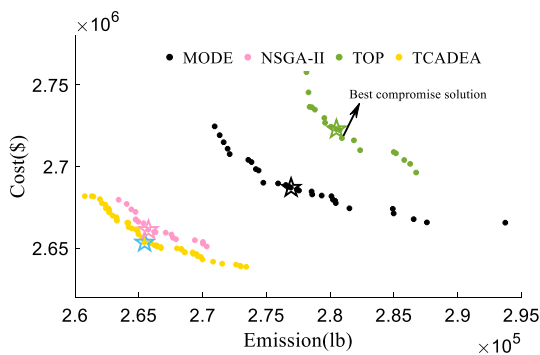


Fig. 15 The PFs of the four test algorithms in Case 4

power, while the heat-only unit takes into account only the heat production power.



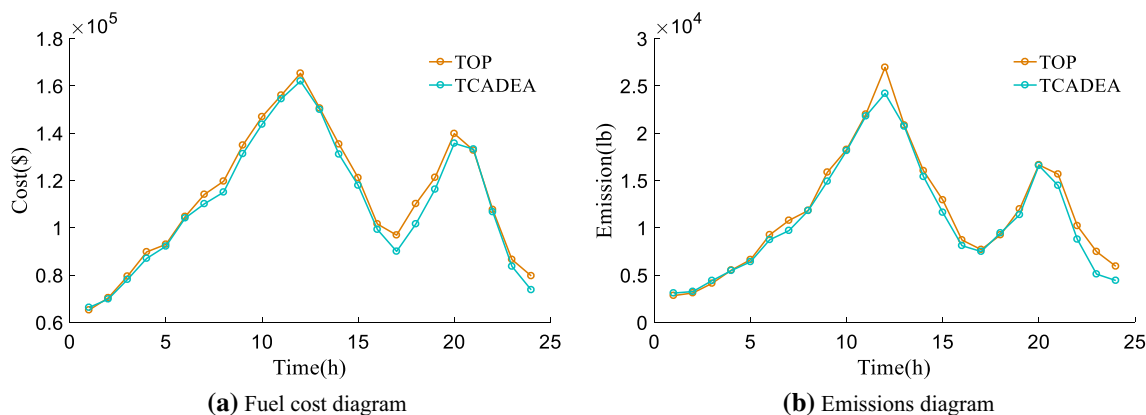


Fig. 16 Fuel cost and emission diagrams for the best compromise solution in Case 4

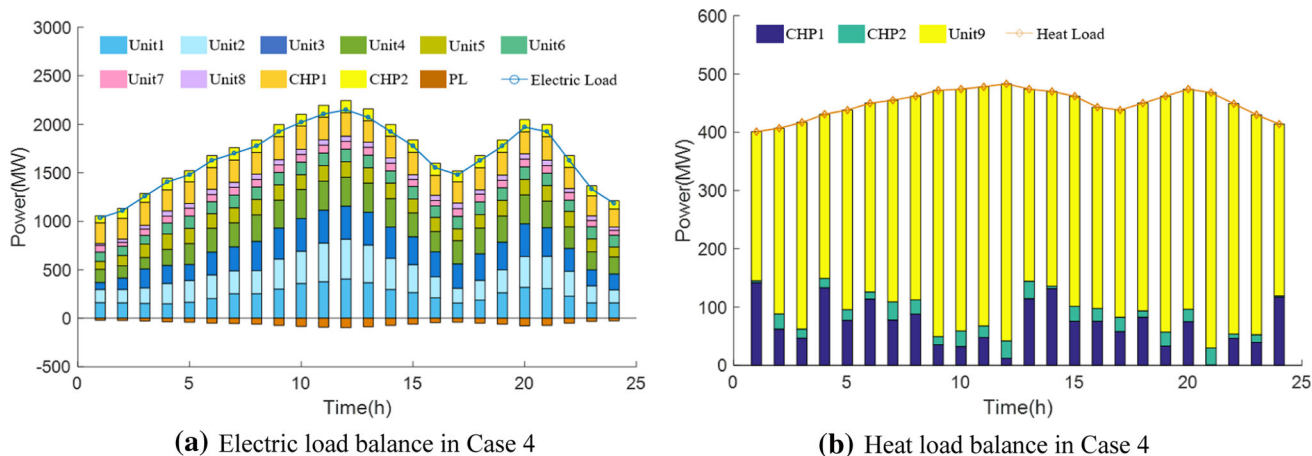


Fig. 17 Output power of each unit in the best compromise solution of Case 4

MODE, NSGA-II, and TOP, respectively. Due to the uncertainty of electricity consumption at the customer side, the load at different times will have errors with the predicted load, which will lead to deviations from the actual situation when using the predicted load data to solve the CEED and CHPEED problems in this paper. In addition, for the optimal set of Pareto solutions obtained, we will focus on automatic selection techniques to select the best compromise solution from the Pareto front.

**Acknowledgements** This work is supported by Hunan Provincial Natural Science Foundation of China (No. 2020JJ4587), Guangdong Basic and Applied Basic Research Foundation (No. 2019A1515110423), Degree & Postgraduate Education Reform Project of Hunan Province (No. 2019JGYB115), Scientific Research Project of Hunan Provincial Department of Education (No. 21C0922), Open Fund Project of Fujian Provincial Key Laboratory of Data Intensive Computing (No. BD202004), Open Fund Project of Key Laboratory of Advanced Perception and Intelligent Control of High-end Equipment of Ministry of Education (No. GDSC202020), and Open Fund Project of Sichuan Key Laboratory of vehicle measurement, control and safety (No. QCCK2021-006).

### Declaration

**Conflict of interest** The authors declare that they have no conflict of interest.

### References

- Muhyaddin, R.; Abdullah, A.; Hussain, B.; Saad, M.; Ziad, M.A.; Shady, H.E.A.A.; Hany, M.H.; Ahmed, I.O.: Economical-technical-environmental operation of power networks with wind-solar-hydropower generation using analytic hierarchy process and improved grey wolf algorithm. *Ain Shams Eng. J.* **12**(3), 2717–2734 (2021)
- Rizk, M.R.; Hala, M.A.M.; Ragab, A.E.; Shady, H.E.A.A.; Adel, E.: A new sine cosine optimization algorithm for solving combined non-convex economic and emission power dispatch problems. *Lnt. J. Energy Convers.* **5**(6), 180–192 (2017)
- Karlsson, J.; Brunzell, L.; Venkatesh, G.: Material-flow analysis, energy analysis, and partial environmental-LCA of a district-heating combined heat and power plant in Sweden. *Energy* **144**(1), 31–40 (2018)
- Basu, M.: Group search optimization for combined heat and power economic dispatch. *Electr. Power Energy Syst.* **78**, 138–147 (2016)

5. Nazari-Heris, M.; Mohammadi-Ivatloo, B.; Gharehpetian, G.B.: A comprehensive review of heuristic optimization algorithms for optimal combined heat and power dispatch from economic and environmental perspectives. *Renew. Sustain. Energy Rev.* **81**(2), 2128–2143 (2018)
6. Niknam, T.; Azizipanah-Abarghoee, R.; Roosta, A.; Amiri, B.: A new multi-objective reserve constrained combined heat and power dynamic economic emission dispatch. *Energy* **42**(1), 530–545 (2012)
7. Murugan, R.; Mohan, M.R.; Christober Asir Rajan, C.; Deiva Sundari, P.; Arunachalam, S.: Hybridizing bat algorithm with artificial bee colony for combined heat and power economic dispatch. *Appl. Soft Comput.* **72**, 189–217 (2018)
8. Zou, D.X.; Li, S.; Kong, X.Y.; Ouyang, H.B.; Li, Z.Y.: Solving the combined heat and power economic dispatch problems by an improved genetic algorithm and a new constraint handling strategy. *Appl. Energy* **237**, 646–670 (2019)
9. Haghrah, A.; Nazari-Heris, M.; Mohammadi-ivatloo, B.: Solving combined heat and power economic dispatch problem using real coded genetic algorithm with improved Mühlenbein mutation. *Appl. Therm. Eng.* **99**, 465–475 (2016)
10. Sakthivel, V.P.; Sumanb, M.; Sathiyac, P.D.: Combined economic and emission power dispatch problems through multi-objective squirrel search algorithm. *Appl. Soft Comput. J.* **100**, 106950 (2021)
11. Zhan, J.P.; Wu, Q.H.; Guo, C.X.; Zhou, X.X.: Fast lambda-iteration method for economic dispatch. *IEEE Trans. Power Syst.* **29**(2), 990–991 (2014)
12. Chen, S.D.; Chen, J.F.: A direct Newton–Raphson economic emission dispatch. *IEEE Trans. Power Syst.* **25**(5), 411–417 (2003)
13. Guo, T.; Henwood, M.I.; Ooijen, M.: An algorithm for combined heat and power economic dispatch. *IEEE Trans. Power Syst.* **11**(4), 1778–1784 (1996)
14. Jeffrey, O.A.; Absalom, E.E.; Laith, A.: Dwarf mongoose optimization algorithm. *Comput. Methods Appl. Mech. Eng.* **391**, 114570 (2022)
15. Laith, A.; Mohamed, A.E.; Putra, S.; Zong, W.G.; Amir, H.G.: Reptile Search Algorithm (RSA): a nature-inspired meta-heuristic optimizer. *Expert Syst. Appl.* **191**, 116158 (2022)
16. Laith, A.; Ali, D.; Seyedali, M.; Mohamed, A.E.; Amir, H.G.: The arithmetic optimization algorithm. *Comput. Methods Appl. Mech. Eng.* **376**, 113609 (2021)
17. Chang, C.S.; Fu, W.: Stochastic multiobjective generation dispatch of combined heat and power systems. *IEE Proc. Gener. Transm. Distrib.* **145**(5), 583–591 (1998)
18. Zou, D.X.; Li, S.; Li, Z.Y.; Kong, X.Y.: A new global particle swarm optimization for the economic emission dispatch with or without transmission losses. *Energy Convers. Manag.* **139**, 45–70 (2017)
19. Koridak, L.A.; Rahli, M.: Optimization of the emission and economic dispatch by the genetic algorithm. *Prz. Elektrotech.* **86**, 363–366 (2010)
20. Abdelaziz, A.Y.; Ali, E.S.; Abd Elazim, S.M.: Flower pollination algorithm to solve combined economic and emission dispatch problems. *Eng. Sci. Technol. Int. J.* **19**(2), 980–990 (2016)
21. Karakonstantis, I.; Vlachos, A.: Ant colony optimization for continuous domains applied to emission and economic dispatch problems. *J. Inf. Optim. Sci.* **36**(1–2), 23–42 (2015)
22. Secui, D.C.: Large-scale multi-area economic/emission dispatch based on a new symbiotic organisms search algorithm. *Energy Convers. Manag.* **154**, 203–223 (2017)
23. Benasla, L.; Belmadani, A.; Rahli, M.: Spiral optimization algorithm for solving combined economic and emission dispatch. *Electr. Power Energy Syst.* **62**, 163–174 (2014)
24. Sharifi, S.; Sedaghat, M.; Farhadi, P.; Ghadimi, N.; Taheri, B.: Environmental economic dispatch using improved artificial bee colony algorithm. *Evol. Syst.* **8**, 233–242 (2017)
25. Basu, M.: Combined heat and power economic emission dispatch using nondominated sorting genetic algorithm-II. *Electr. Power Energy Syst.* **53**(1), 135–141 (2013)
26. Shaabani, Y.; Seifi, A.R.; Kouhanjani, M.J.: Stochastic multi-objective optimization of combined heat and power economic/emission dispatch. *Energy* **141**, 1892–1904 (2017)
27. Sun, J.Z.; Deng, J.H.; Li, Y.: Indicator & crowding distance-based evolutionary algorithm for combined heat and power economic emission dispatch. *Appl. Soft Comput. J.* **90**, 106158 (2020)
28. Li, Y.; Wang, J.L.; Zhao, D.B.; Li, G.Q.; Chen, C.: A two-stage approach for combined heat and power economic emission dispatch: Combining multi-objective optimization with integrated decision making. *Energy* **462**, 237–254 (2018)
29. Sundaram, A.: Multiobjective multi-verse optimization algorithm to solve combined economic, heat and power emission dispatch problems. *Appl. Soft Comput. J.* **91**, 106195 (2020)
30. Shi, B.; Yan, L.X.; Wu, W.: Multi-objective optimization for combined heat and power economic dispatch with power transmission loss and emission reduction. *Energy* **56**, 135–143 (2013)
31. Naderi, E.; Pourakbari-Kasmaei, M.; Abdi, H.: An efficient particle swarm optimization algorithm to solve optimal power flow problem integrated with FACTS devices. *Appl. Soft Comput. J.* **80**, 243–262 (2019)
32. Anand, H.; Narang, N.; Dhillon, J.S.: Multi-objective combined heat and power unit commitment using particle swarm optimization. *Energy* **172**, 794–807 (2019)
33. Murugana, R.; Mohan, M.R.; Christober Asir Rajan, C.; Deiva Sundari, P.; Arunachalam, S.: Hybridizing bat algorithm with artificial bee colony for combined heat and power economic dispatch. *Appl. Soft Comput.* **72**, 189–21 (2018)
34. Storn, R.; Price, K.: Differential evolution: a simple and efficient heuristic for global optimization over continuous spaces. *J. Global Optim.* **11**, 341–359 (1997)
35. Zitzler, E.; Deb, K.; Thiele, L.: Comparison of multiobjective evolutionary algorithms: empirical results. *Evol. Comput.* **8**(2), 173–195 (2000)
36. Liu, Z.Z.; Wang, Y.: Handling constrained multiobjective optimization problems with constraints in both the decision and objective spaces. *IEEE Trans. Evol. Comput.* **23**(5), 870–884 (2019)
37. Riquelme, N.; Von Lücken, C.; Baran, B.: Performance metrics in multiobjective optimization. In: 2015 Latin American Computing Conference (CLEI), Arequipa, pp. 1–11 (2015)
38. Basu, M.: Economic environmental dispatch using multi-objective differential evolution. *Appl. Soft Comput.* **11**, 2845–2853 (2011)
39. Güvenç, U.; Sönmez, Y.; Duman, S.; Yörükeren, N.: Combined economic and emission dispatch solution using gravitational search algorithm. *Sci. Iran.* **19**(6), 1754–1762 (2012)